IEEE Access
Multidisciplinary ⋮ Rapid Review ⋮ Open Access Journal

Received July 5, 2020, accepted July 15, 2020, date of publication July 20, 2020, date of current version August 4, 2020.

Digital Object Identifier 10.1109/ACCESS.2020.3010576

Analysis and Design of Novel High Speed Permanent Magnet Machine Considering Magnet Eddy Current Loss

HAMID ALI KHAN[1], FAISAL KHAN[1], NASEER AHMAD[2], AND JONG-SUK RO[3]

[1]Department of Electrical and Computer Engineering, COMSATS University Islamabad–Abbottabad, Abbottabad 22060, Pakistan
[2]Faculty of Information and Communication Technology, Balochistan University of Information Technology, Engineering and Management Sciences (BUITEMS), Quetta 87300, Pakistan
[3]School of Electrical and Electronics Engineering, Chung-Ang University, Seoul 06974, South Korea

Corresponding author: Jong-Suk Ro (jongsukro@gmail.com)

This work was supported in part by the Basic Science Research Program through the National Foundation of Korea funded by the Ministry of Education under Grant 2016R1D1AB01008058, and in part by the Human Resources Development of the Korea Institute of Energy Technology Evaluation and Planning (KETEP) Grant funded by the Korean Government Ministry of Trade, Industry, and Energy under Grant 20184030202070.

ABSTRACT In high speed permanent magnet (HSPM) machines, the computation of magnet eddy current loss is essential as these losses significantly affect the temperature of the permanent magnet (PM) and electromagnetic performance and can result in irreversible demagnetization of the PM. Several techniques have been adopted to minimize the eddy current loss of the PM; however, superior performance has not been achieved yet. In this paper, the design characteristics of the HSPM machine are analyzed. The PM is covered by a titanium sleeve to retain the PM on the rotor and to further reduce the eddy current loss of the magnet. The undesirable harmonics of the airgap flux density are minimized, which reduces the eddy current loss in the solid PM and rotor. Two existing models, with and without auxiliary slots, are examined and compared with the proposed design having a titanium-based retaining sleeve. The analysis reveals that the eddy-current loss, cogging torque, and iron losses of the PM are reduced by 82%, 73%, and 44.7%, respectively, in the proposed model; however, a marginal increase is observed in the average rated torque profile and open circuit flux linkage.

INDEX TERMS Auxiliary slot, eddy current losses, finite element analysis, high speed machine, iron loss, permanent magnet, sleeve, spatial harmonics.

I. INTRODUCTION

High speed permanent magnet (HSPM) machines have become significantly popular in recent times owing to their utilization in various applications, such as automotive and aerospace applications, gas turbines, air blowers, and spindles. A permanent magnet (PM) synchronous machine is a suitable choice because of its small size, high efficiency, and high power density [1], [2]. Since the introduction of high power PMs, several papers have been published on PMs employed in models that are designed for high speed applications [3]–[5].

However, several challenges exist in the manufacturing of HSPM machines as field windings are replaced by PMs. In comparison with other machines, the core loss of the PM machine constitutes a high proportion of the total loss. A proper design for the high speed machine is necessary because the rotor body and its components can be easily damaged owing to the high eddy current loss [6]. For better performance and high efficiency, precise estimation of the core loss for a PM machine is crucial. Usually, the eddy current losses are small when compared to other losses; however, due to comparatively inefficient heat dissipation system, the heat remains in the PM rotor, which can heat the PM and result in irreversible demagnetization of the magnet. In PM machines, the eddy current loss is produced by asynchronous harmonics; such harmonics are spatial harmonics in a stator magnetomotive force distribution and time harmonics in a stator non-sinusoidal current waveform, which significantly affect the performance of the machine. In PM machines,

The associate editor coordinating the review of this manuscript and approving it for publication was Atif Iqbal.

the rotor losses are caused by a permeance variation of the airgap due to the slotting of the stator. When pulse width modulation (PWM) inverters are used for the excitation of PM machines, eddy current losses are produced by the switching harmonics of the PWM inverter [7], [8]. Hence, it is essential to diminish the spatial and time harmonics of the machine. There are significantly strong mechanical and thermal constraints for high speed machines that restrict their power and speeds limits [9], [10]. For HSPM machines, the eddy current loss computation is very important, as it considerably increases with the speed of the machine and influences the magnet temperature as well as the efficiency and output torque; moreover, this loss can demagnetize the PMs.

The eddy current loss in a surface-mounted PM machine is greater than that of interior PM (IPM) motors owing to the large stator-slot openings. Nevertheless, in IPM motors, the magnetic path changes because of the permeance distribution of the rotor with rotation, which causes magnet eddy current losses [11], [12].

In the last decade, several researchers have focused on the reduction of magnet eddy current loss. To suppress the eddy current loss of rotor, different machine models were proposed. A possible solution to this problem is the optimization of winding, which is the most important factor for these machines because a suitable winding configuration can minimize the spatial harmonics of the armature field (AF) efficiently [13]–[15]. Rotor shape optimization is the best choice to diminish the eddy current loss and cogging torque while increasing the power density and efficiency of the machine; however, these approaches have a disadvantage of a low winding factor; consequently, a high copper loss occurs for the same output torque [16].

Rotor eddy current losses are minimized by increasing the length of the airgap; however, it influences the power density of the machine [17]. Skewing and segmentation can also be used to break up the paths of the eddy current, resulting in a reduction in eddy current loss; but the process is complicated, difficult to fabricate, and has a high cost of production [18], [19]. While using the process of segmentation, the magnet eddy current loss reduces in accordance with the number of divisions. However, [20] shows that this rule is applicable only when certain parameters are neglected, such as skin effect, end effect, and uniform magnetic flux density along the width of the PM.

Owing to the return path of the eddy currents in the PM, the eddy current loss is a three dimensional (3D) problem that requires a 3D finite element analysis (FEA) for computation; however, this technique is significantly time consuming. These losses can also be calculated analytically, which is considerably effective but difficult to implement [21]. Several analytical methods including the FEA are limited to two-dimensional (2D) analysis because of the difficulty in calculating the rotor eddy current loss [22]–[24].

Several other methods are used for estimation and reduction of these losses, such as conducting sleeve and copper shielding [25]–[27]; however, these methods increase the total eddy current losses of the rotor. The utilization of PWM is another method to reduce the harmonics of the airgap permeance that cause eddy losses [28]; however, this method only diminishes the time harmonics.

The eddy current loss of the magnet can also be decreased by optimizing the slot opening and its position; however, the reduction was only 15% [29]. The rotor-shape and core optimizations can also reduce the eddy current loss of the PM. Notching in the stator teeth or introducing auxiliary slots (AS) in the stator teeth to minimize the eddy current loss of the PM were proposed by [30], [31], which partially reduced the magnet eddy current losses. However, the amplitude of the spatial harmonics was not minimized.

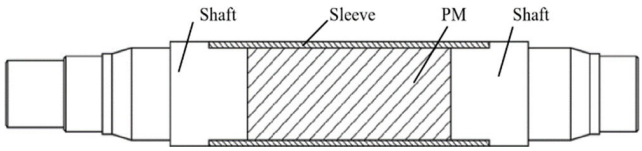

FIGURE 1. Rotor topology with solid permanent magnet.

In [32], [33], certain designs were proposed, in which a solid PM was used and the shaft was replaced by the PM. To protect the PM and link the shafts from both sections, a retaining sleeve is used, as shown in Fig. 1. To retain the PM on the rotor and minimize the eddy current loss of the PM, high strength, highly resistive retaining sleeve materials are used, such as Inconel, stainless steel, titanium, and carbon fiber composite (CFC) [34], [35]. The rotor stress and retaining sleeve thickness must be calculated accurately to stabilize the stress, otherwise the rotor can be critically damaged.

Tensile stress in the magnet is converted to compressive stress by the retaining sleeves; hence, high tensile strength materials are preferred for the sleeve. Nonmetallic and plastic sleeves can minimize the magnet eddy current loss drastically; however, the sleeve is typically thermal resistive and thus resists the heat from the magnets. As the sleeves are directly in contact with the airgap, a further advantage of easy cooling is demonstrated. The distribution of eddy current losses in the rotor is primarily affected by the sleeve conductivity. With the high conductivity of the sleeve, the PM eddy current loss is specifically reduced. To utilize the advantage of this technique, high conductive sleeves are used; however, this results in an increase in the total rotor eddy current losses [25].

This paper proposes a design to diminish the eddy current loss of the PM by using a titanium sleeve over the PM and incorporating AS in the teeth of the stator. The rotor eddy current losses are computed by FEA analytical method for the proposed model. The proposed design is optimized for minimum eddy current loss and a high value of average rated torque.

The paper is organized as follows. In section II, the design methodology for both conventional designs and the proposed design are analyzed. Sections III and IV discuss the analytical calculation of the magnet eddy current and iron

losses, respectively. The open-circuit and short-circuit analyses based on the FEA are examined in section V. In section VI, the effects of different working conditions are investigated for both the conventional and proposed designs. Finally, in section VII, the optimization of the proposed design is presented, and the different parameters of the conventional, proposed, and optimized designs are compared and discussed.

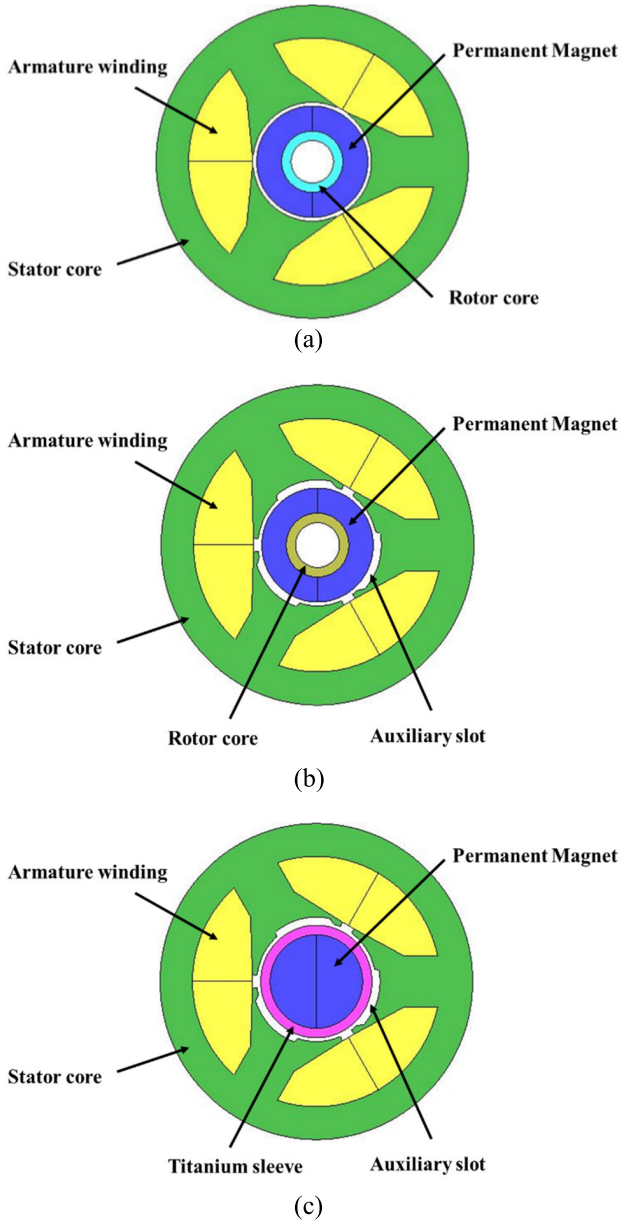

FIGURE 2. Cross-sectional view of (a) conventional model without auxiliary slots (AS), (b) conventional design with AS, and (c) proposed model.

II. DESIGN METHODOLOGY

In this paper, the design study and performance analysis of a two-pole/three slot PM machine are investigated. A two pole/three slot machine with concentrated winding was selected for winding configuration, which can reduce the copper losses and improve the performance of the machine.

TABLE 1. Design parameters.

Number of poles	2	Magnetic material	Nd-Fe-B
Outer diameter of stator	50 mm	Rated current	10 A
Outer diameter of rotor	17 mm	Rated speed	60000 rpm
Height of yoke	5.2 mm	Number of turns	32 turns
Opening of slot	2 mm	Depth of AS	9.540 mm
Length of airgap	0.6 mm	Width of AS	0.549 mm
Diameter of PM	7.08 mm	Axial length	30 mm

The performance of two conventional machines, i.e., without AS and with AS, as shown in Figs. 2 (a), (b), respectively, were analyzed and then compared with the results of the proposed design. The design parameters of the conventional and proposed designs are listed in Table 1. A two pole rotor machine was selected due to the high operating speed of the machine to restrict the fundamental frequency. Instead of a surface-mounted PM, a cylindrical solid PM was used for rotor balance dynamic and ease of manufacturing. In the rotor topology shown in Fig. 1, the sleeve on the PM is mounted through an interference fit. As the critical speed strongly varies according to the bearing span, the mechanical constraints of the design are critical.

For analyzing the source of spatial harmonics in the machine, an analysis of airgap magnetic field is required. Minimizing the spatial harmonics that result in PM eddy current loss, we propose a design that uses a titanium-based retaining sleeve over the PM, as shown in Fig. 2(c). By using the titanium sleeve over the PM, the amplitudes of the airgap flux density harmonics were reduced, and the angle between the AF harmonics and the PM field harmonics was approximately 180 °C, which further reduced the magnet eddy-current loss. The thickness of the sleeve is considered as the outer radius of the proposed model, which is not greater than that of the conventional model. Different materials, such as CFC, copper, and titanium, can be used for the sleeve, which reduces the eddy current loss. The CFC has low flexibility stiffness; consequently, it is not used for the sleeve because of the dependency on bending rigidity, critical speed of the rotor, and low heat-transfer coefficient, which affect the thermal performance of the machine. A copper sleeve can considerably reduce the magnet eddy current loss, but it increases the rotor total eddy current losses; hence, it is not preferred for the sleeve. The critical speed and bending rigidity of the proposed rotor primarily depends on the sleeve; therefore, a high-stiffness titanium material was considered for the sleeve to minimize the magnet eddy-current loss as well as suppress total iron losses of the machine.

III. PROPOSED ANALYSIS OF MAGNET EDDY-CURRENT LOSS

In PM machines, the core loss constitutes a major portion of the total losses compared to other machines. Hence,

for improved performance and high efficiency of the PM machines, an efficient computation of core losses is crucial. In the PM machines, magnet eddy-current losses are usually neglected owing to the high resistivity of the ferrite magnets; in contrast, the rare-earth magnets such as Nd-Fe-B have lower resistivity. Hence, it is essential to compute these losses as they can demagnetize the PM and boost the temperature of the rotor, if Nd-Fe-B magnets are heated to a high temperature, such as 120 °C.

A. EDDY-CURRENT LOSS PER UNIT OF THE MAGNET VOLUME

The current density in a magnet is computed by the second Maxwell's equation [36]:

$$\oint E.ds = -\frac{d}{dt}\iint B.d\alpha \tag{1}$$

The strength of electric field can be calculated as the product of magnet resistivity and current density.

$$E = \rho_m.J. \tag{2}$$

Hence, the current density can be calculated as

$$J(x) = \frac{x}{\rho_m}\frac{dB}{dt}. \tag{3}$$

The eddy current losses per unit magnet volume can be calculated as

$$k_m = \frac{1}{b_m}\int_{-b_m/2}^{b_m/2} \rho_m J^2(x)dx = \frac{b_m^2}{12\rho_m}\left(\frac{dB}{dt}\right)^2. \tag{4}$$

Losses in the k-th magnet caused by the magnetic flux density can be computed as

$$B_k = B(\alpha_k) = \hat{B}\cos(p(\alpha_k - \beta)). \tag{5}$$

In (4), by replacing the flux density, the eddy current loss per unit volume of the PM in the k-th magnet can be determined as:

$$k_{m,k} = \frac{b_m^2}{12\rho_m}\left(\frac{d}{dt}\left\{\hat{B}\cos\left(p\left(\alpha_{k-\beta}\right)\right)\right\}\right)^2 \tag{6}$$

The total magnet eddy current loss is equal to the sum of the magnet losses in total number of magnets N_m:

$$P_m = l_s l_m b_m \sum_{k=1}^{N_m}\frac{b_m^2}{12\rho_m}\left(\frac{d}{dt}\left\{\hat{B}\cos(p(\alpha_k - \beta))\right\}\right) \tag{7}$$

where:

l_m : thickness of the magnet,
l_s : motor axial length,
b_m : width of the magnet,
α_k : magnet k-th axis aligned with the rotor coordinates,
ρ_m : magnet resistivity,
β : function of time,
P : motor pole pairs,
B : magnet flux density.

The estimated eddy-current loss of the PM is calculated as follows:

$$P_m \approx \frac{V_m b_m^2 \hat{B}_m^2 \omega^2}{12\rho_m} \tag{8}$$

where:

ω : frequency,
ρ_m : magnetic resistivity,
b_m : width of the magnet,
V_m : volume of the magnet,
B_m: airgap flux density.

IV. ANALYSIS OF IRON LOSS

The iron loss includes the dynamic and hysteresis losses, i.e.,

$$\mathcal{P}F_e = \mathcal{P}_d + \mathcal{P}_h \tag{9}$$

where $\mathcal{P}_d$ is the dynamic loss and $\mathcal{P}_h$ is the hysteresis loss.

The hysteresis loss is produced by the discontinuous magnetization process and measured by multiplying the area of the B–H loop under a DC hysteresis test with the frequency, where B indicates the magnetic flux density and H indicates the magnetic field strength. The dynamic loss is the Joule loss produced by the flow of eddy current.

The iron losses are calculated using the model presented by [37]–[38], which depends on the flux density and frequency.

$$\mathcal{P}_{Fe} = K_h(f, B_m) f B_m^2 + K_e(f, B_m) f^2 B_m^2 \tag{10}$$

Here:

K_h : hysteresis Loss coefficient,
f : frequency,
B_m : flux density,
K_e : eddy loss coefficient.

V. PERFORMANCE ANALYSIS OF THE PROPOSED DESIGN BASED ON FINITE ELEMENT ANALYSIS (FEA)

To recognize the source of the spatial harmonics in the two-pole/three-slot machine, an analysis of the airgap magnetic field is required. The airgap flux density harmonics were calculated using FEA. The performance analysis of the open-circuit conditions included the investigation of the no-load flux linkage, cogging torque, and coil test analyses. The short-circuit conditions such as average eddy-current loss and rated torque were also examined.

A. FLUX LINKAGE

The flux linkages of the coils in all the machines were observed and the U-phase flux of each machine is illustrated in Fig. 3. In the proposed design, the flux linkage was marginally less than that of the conventional models owing to the incorporation of the sleeve in the proposed model. The flux linkage of the proposed design was reduced by 20% from that of the conventional designs.

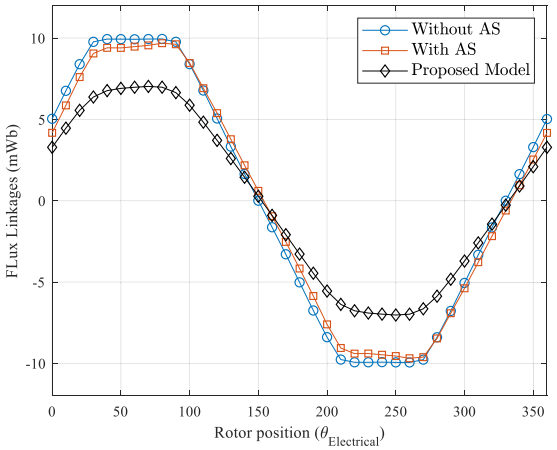

FIGURE 3. Comparison of flux linkage.

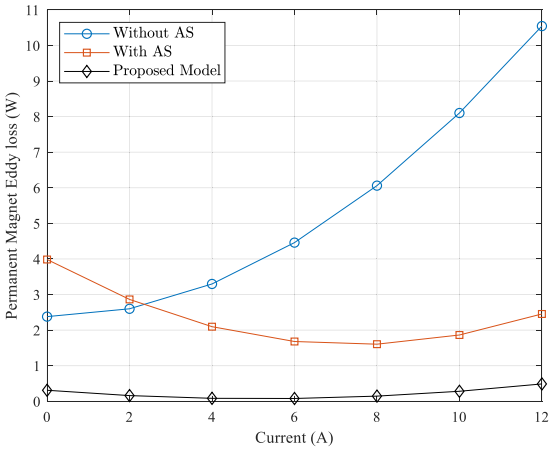

FIGURE 5. Comparison of magnet eddy-current loss.

B. COGGING TORQUE

Cogging torque is the interconnection force between the slots of the stator and the rotor PM, which can affect the operation of electrical motors. It is calculated at no-load conditions. For better operation of a motor, it is essential that the motor should exhibit a low cogging torque. Fig. 4 shows the cogging torque at various rotor positions, which clearly indicates that in the proposed design the cogging torque is lesser than that of the conventional machines by 69%; this demonstrates the effectiveness of the proposed design.

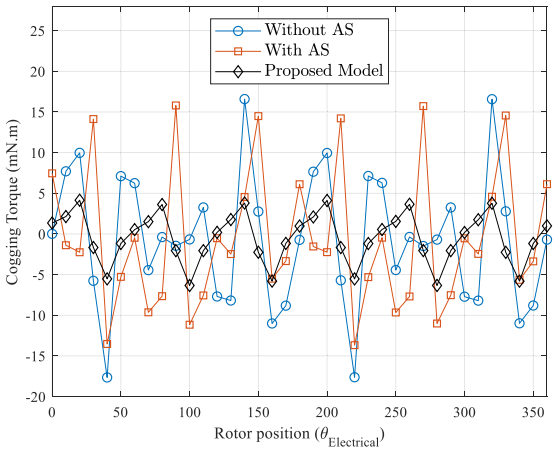

FIGURE 4. Cogging torque comparison between the conventional and proposed designs.

C. MAGNET EDDY LOSSES

It is worth mentioning that the sources of eddy current losses are the spatial and time harmonics. The airgap flux density analysis was performed to determine the spatial harmonics. The harmonics in the proposed machine were significantly less when compared to that of the conventional models. The volume of the magnet was equal to that used in the conventional models; in contrast, the shaft of the proposed model was truncated by the PM, and a retaining sleeve was used over it to maintain the PM between the shafts. Fig. 5 shows that the average eddy current loss of the magnet in the proposed design is moderately less than that in the conventional designs throughout the loaded conditions. The PM eddy current loss in the conventional design without AS increased with the increasing current amplitude, whereas the losses in the conventional design with AS initially decreased with the increasing current amplitude; however, the losses increased after the rated condition. In the proposed model, the magnet eddy current loss demonstrated the same behavior as that of the conventional model with AS. However, the losses in the proposed model were significantly less throughout different working conditions; at the rated condition, i.e., 10 A of current, the magnet eddy current loss was reduced by 82% when compared to the conventional model with AS. Hence, the proposed model is considerably effective for the reduction of the magnet eddy current loss.

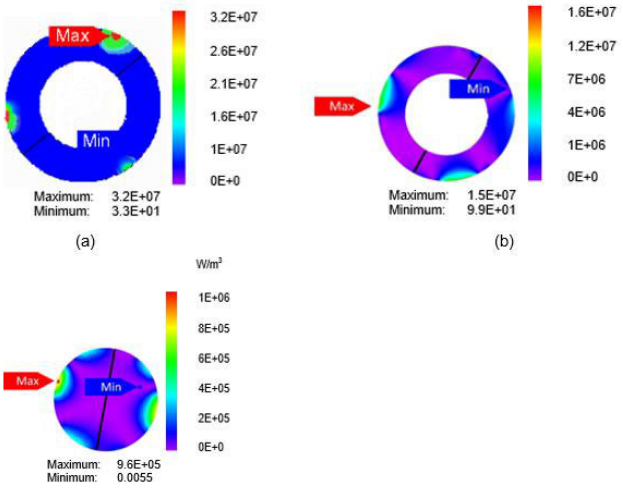

FIGURE 6. Two-dimensional distribution of eddy-current losses in the magnet.

To justify the effectiveness of the proposed design, a 2D FEA was performed. Figs. 6 (a), (b), and (c) show the 2D FEA

results of the magnet eddy current loss distribution in the PM of the conventional designs (without AS and with AS) and that of the proposed design, respectively. The figure clearly illustrates that by using the titanium sleeve over the PM, the eddy current loss of the magnet, in comparison with that of conventional designs, is reduced considerably.

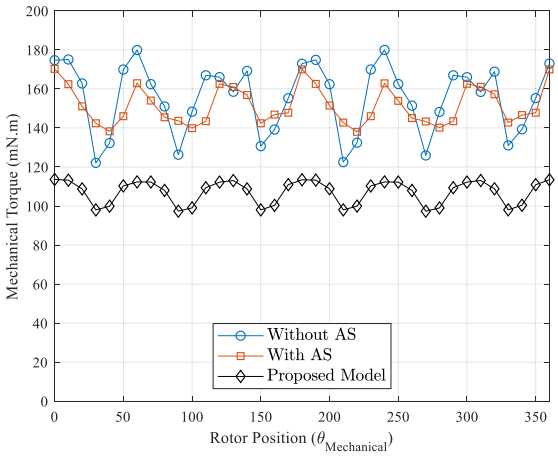

FIGURE 7. On-load rated toque comparison.

D. AVERAGE TORQUE

The rated torque profile of the machines at 10 A of current is shown in Fig. 7. The figure illustrates that in the proposed model, the rated torque marginally decreases, and demonstrating low torque ripples. The rated torque was decreased by 19.9% in the proposed model when compared to the conventional design having AS. The reduction of average torque primarily depends on the width of the sleeve; as the sleeve width increases, the torque decreases. The effect of sleeve width on average torque is discussed later in this paper.

E. IRON LOSSES

Iron losses have a major contribution in the overall losses of the machine. The performance of the machine is significantly affected by iron losses due to which the flux densities in the cores of the stator and rotor vary. By implementing the proposed model, the flux density variation was reduced because of the consumption of the rotor core. Owing to the high armature reaction, which was caused by the increasing electrical loading, the iron losses were increased to a certain level. Fig. 8 shows that the iron losses of the proposed design is less than that of both the conventional models, i.e., without AS and with AS, because the rotor of the conventional design having AS was replaced by the new rotor design (solid PM and a titanium sleeve).

To examine the spatial harmonics in detail, the airgap flux density harmonics were simulated at different working conditions. The second (2^{nd}) spatial harmonic was considered for analysis. Fig. 9 shows the 2^{nd} harmonics of the airgap flux density of the armature and PM fields of the conventional and proposed designs. Using the frozen permeability method,

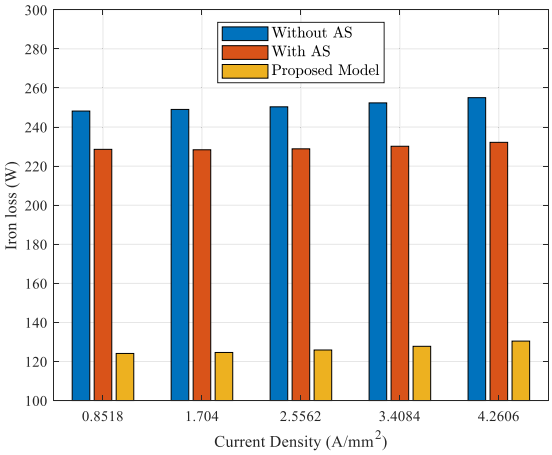

FIGURE 8. Iron losses vs. current density.

the harmonics of airgap flux density at various working conditions were analyzed. It can be noticed that the other harmonics have a small influence on the losses. The phase difference (PD) between the AF and the PM field was less than 180° in the conventional machines, which partially minimized the asynchronous harmonics of the airgap flux density. Fig. 9 also illustrates that the amplitude of the PM field is high in the conventional models, which resulted in the high eddy current loss of the magnet.

The amplitude of the 2^{nd} harmonic in the proposed machine was not zero, but it was lesser than that of the conventional models; consequently, the eddy current loss of the magnet significantly decreased. Here, only the 2^{nd} harmonic is analyzed; however, these principles can be applied to other harmonics as well for analysis. The amplitude of the harmonics caused by the AF increased with different input currents; in contrast, the PD between the AF and the PM field harmonics was approximately the same throughout the different working conditions.

VI. EFFECT OF DIFFERENT WORKING CONDITIONS

The performance of the machine at rated working condition was discussed in the previous section. However, the working conditions can change; therefore, an analysis at different working conditions is required. Figs. 10 (a), (b), (c) and Figs. 11 (a), (b), (c) illustrate the eddy current losses of the PM and the loaded torque in the conventional models (without AS and with AS) and in the proposed model, respectively, at various working conditions. It can be concluded that the conventional designs have considerably higher eddy current losses corresponding to the increase in the amplitude of the current; moreover, the angle of current has a small influence on the losses. Increasing the current amplitude demonstrated a small effect on the eddy current loss of the PM in the proposed model. Therefore, magnet eddy current losses in the proposed model were significantly lesser than that of the conventional designs without AS and with AS at different working conditions. The eddy current loss of the magnet in

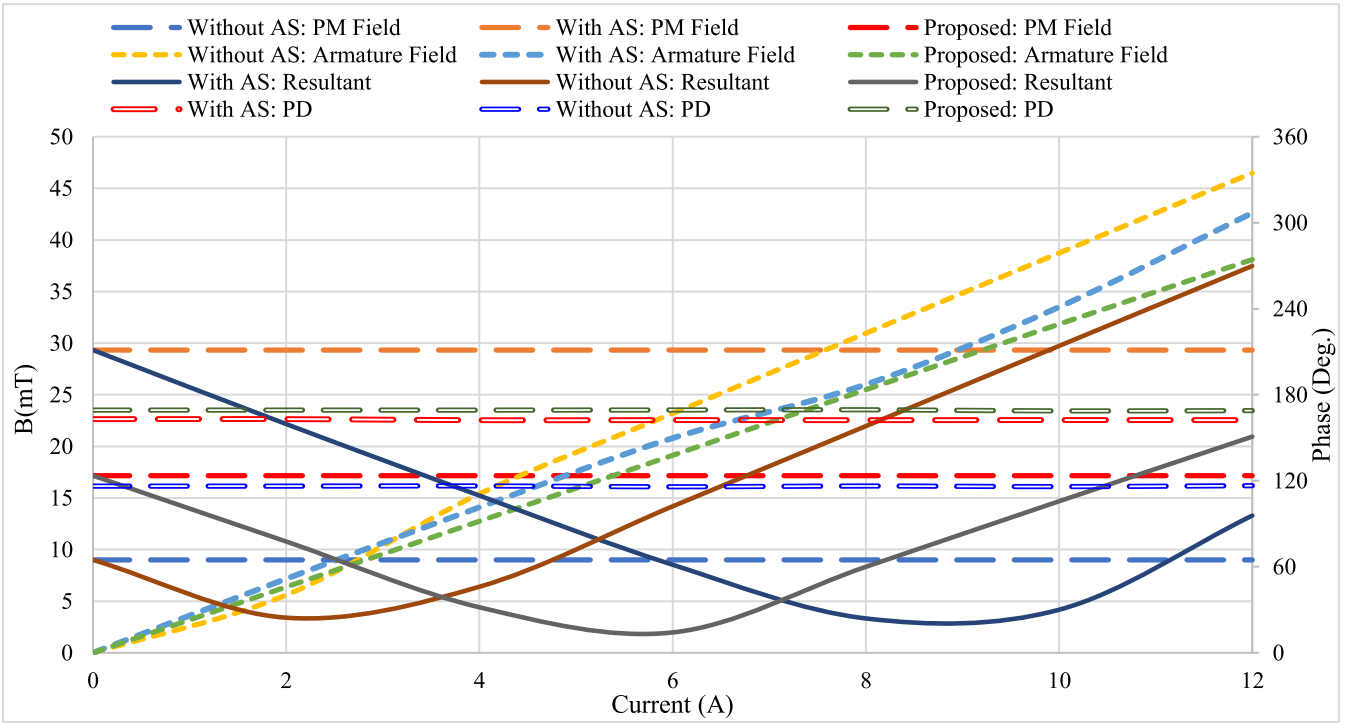

FIGURE 9. 2nd harmonic of airgap flux density at different current values.

the proposed model was decreased by 77.6% when compared with that of the conventional model with AS at a current of 15 A and an angle equal to 90°. However, the torque in the proposed model was reduced when compared with the conventional models.

The average rated torque in the proposed design was less than that of the conventional designs; therefore, the optimization of the proposed design was performed by a deterministic algorithm, which is discussed later in this paper.

VII. OPTIMAL DESIGN OF THE PROPOSED MODEL

When compared to the conventional designs, the magnet eddy current loss in the proposed machine was significantly smaller; further, the rated torque of the proposed design was also less than that of the conventional machines. To improve the torque of the proposed model, a deterministic optimization procedure was adopted.

Using the deterministic optimization, the yoke and stator pole widths were optimized with the constraint that the yoke and pole are not saturated. As the pole and yoke widths reduced when optimized, the area of the stator slots also increased. Increasing the area of the stator slots resulted in variations in the electrical loading of the machine, which further increased the number of turns. Equation 11 is used to calculate the accurate number of turns for the armature coil. The motor filling factor was considered as 0.5; the current density has a fixed value, which was determined from the conventional machines.

$$N_a = \frac{J_a S_a \alpha}{I_a}, \tag{11}$$

where:

N_a : number of turns,
J_a : current density,
S_a : Slot area,
α : filling factor,
I_a : input current.

A. OPTIMAL DESIGN OF YOKE

The influences of yoke size on the eddy current losses and average torque are shown in Fig. 12. The relation between the yoke size and both eddy current losses and rated torque is inversely proportional, i.e., as the size of yoke increases, the eddy current losses and rated torque decrease. Fig. 12 indicates that the yoke size has a small effect on the eddy current loss of the magnet, which increases from 0.3 W to 0.42 W corresponding to the decrease in the yoke size from 5.2 mm to 4 mm; in contrast, the effect on the sleeve eddy current loss is marginally high; it increases from 1.85 W to 2.75 W. Conversely, the average rated torque decreases from 127.5 mN·m to 105.5 mN·m corresponding to the increase in the width of the yoke in the proposed design.

B. OPTIMAL DESIGN OF POLE

The eddy current losses and rated torque decrease as the width of the stator pole increases. Fig. 13 indicates that the width

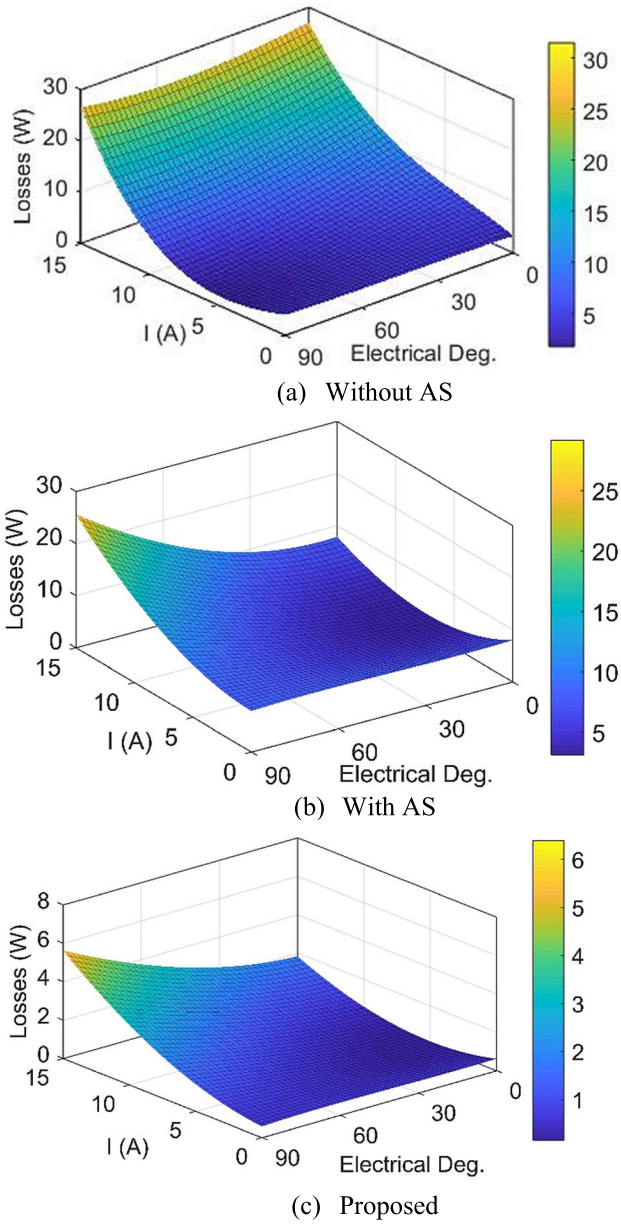

FIGURE 10. Magnet eddy current loss at different rated conditions.

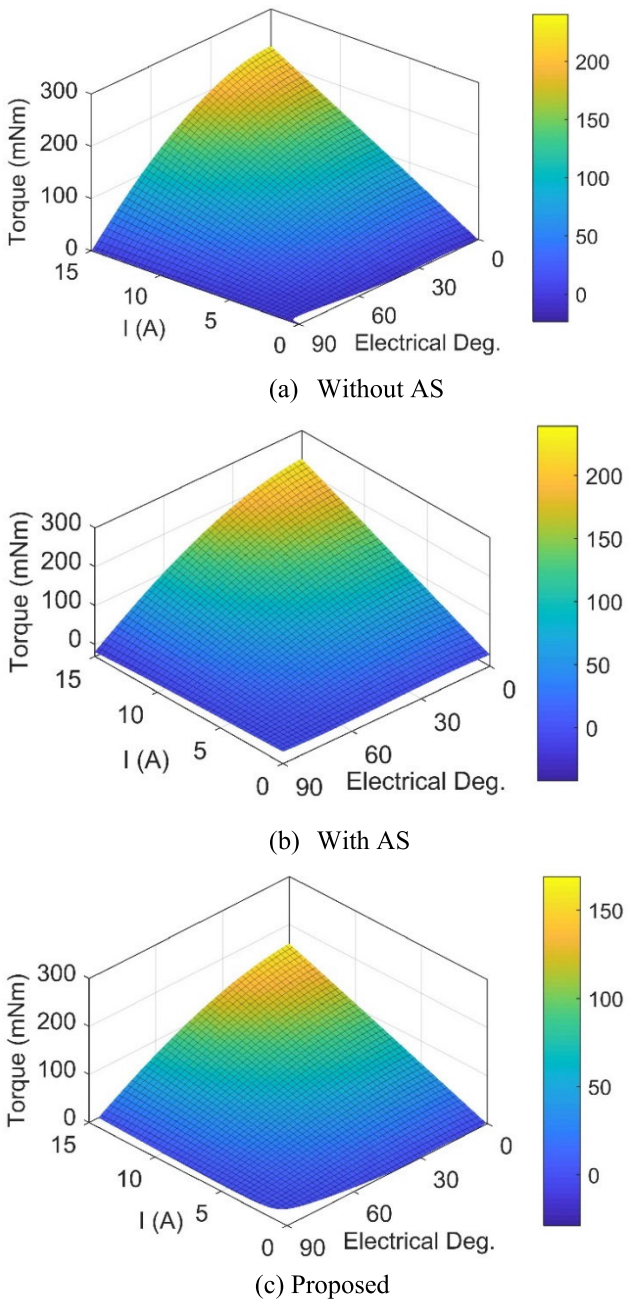

FIGURE 11. Average torque at different rated conditions.

of the pole has a considerable effect on the eddy current loss of the magnet, which decreases from 0.55 W to 0.4 W. Meanwhile, the eddy current loss of the sleeve diminishes from 2.75 W to 2.33 W. The average rated torque of the proposed machine does not decrease linearly with the pole width; however, the effect of the pole width is moderately high as it reduces the value of rated torque from 138 mN·m to 118 mN·m.

The optimized design is shown in Fig. 14 and its dimensions are listed in Table 2.

No-load and loaded analyses of the optimized design was performed and the peak-to-peak values of the results are listed in Table 3. The flux linkage of the optimized design increased by 15% and 30% when compared with the conventional model with AS and the proposed design, respectively. The cogging torque of the optimized design increased marginally when compared with the initially proposed model; however,

TABLE 2. Design parameters.

Pole width	5 mm
Yoke size	4 mm
Sleeve width	1.3 mm
Rated current density	4.45 A/mm^2

TABLE 3. Comparison of different parameters of all models.

Parameters	Without AS	With AS	Proposed	Optimized
Flux linkages	18 mWb	17 mWb	14 mWb	20 mWb
Cogging torque	20 mN·m	23 mN·m	6.2 mN·m	7.4 mN·m
Magnet eddy-current losses	8.15 W	1.86 W	0.28 W	0.55 W
Rated torque	152.6 mN·m	149.7 mN·m	118.3 mN·m	157 mN·m
Iron losses	251 W	230 W	127.7 W	177.86 W

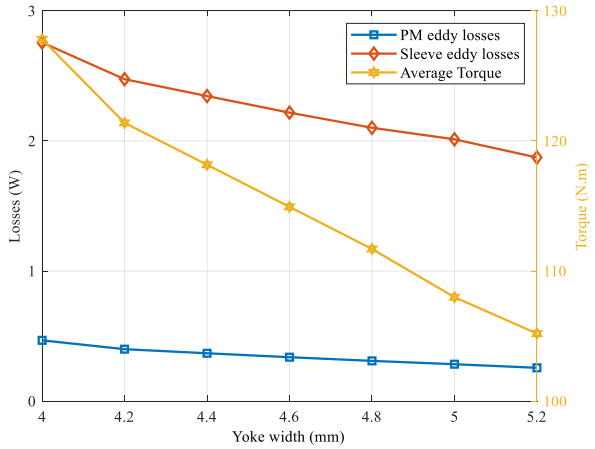

FIGURE 12. Yoke size vs. eddy current losses and rated torque.

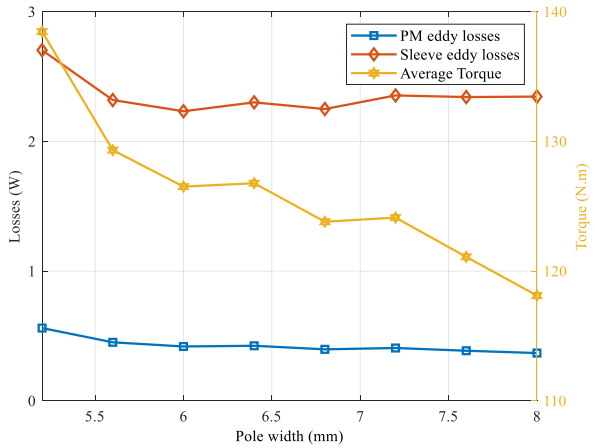

FIGURE 13. Pole width vs. eddy current losses and torque.

it was still lesser than that of the conventional designs. At rated condition, i.e., when current was equal to 10 A, the optimized design demonstrated a moderately high average torque, i.e., it increased by 24.6% when compared with the initial design. Conversely, the optimized design demonstrated marginally higher iron losses than the initial design owing to the high electrical loading; however, it was still less than that of the conventional designs.

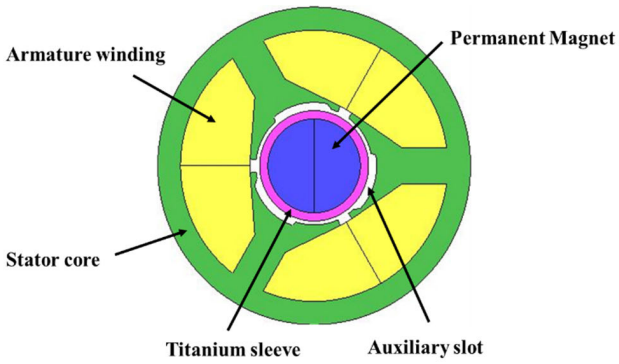

FIGURE 14. Optimized model.

VIII. COMPARISON OF FEA AND ANALYTICAL RESULTS

The effectiveness of the proposed method was validated by comparing the FEA of the proposed machine with the analytically calculated values of the magnet eddy current and iron losses, as listed in Table 4. The magnet eddy current loss for the conventional designs with AS and without AS as well as that for the proposed and optimized design were calculated using (8), whereas the FEA values were determined by finite element simulation. The difference between the FEA and analytical values were 36.3%, 22.2%, and 22.5% for the conventional design with AS, proposed design, and optimized design, respectively. Iron losses, which depend on the frequency and magnetic flux density, were calculated according to (10). The analytically computed values of the iron losses for the conventional models with AS and proposed model as well as that for the optimized model were less than the simulated values by 30 W, 1.7 W, and 15.4 W, respectively. It can be determined from Table 4 that the FEA simulation results closely agree with the analytically calculated values, and the difference between the FEA results and analytically calculated values is minimal. Further, good predictions of magnet eddy current and iron losses are obtained through the FEA simulation.

TABLE 4. Comparison between finite element analysis and calculated values of the proposed analytical method.

Parameters	Conventional without AS		Conventional with AS		Proposed design		Optimized design	
	FEA value	Calculated value by PAM	FEA value	Calculated value by PAM	FEA value	Calculated value by PAM	FEA value	Calculated value by PAM
Magnet eddy-current losses	8.15 W	9.6 W	1.86 W	2.92 W	0.28 W	0.36 W	0.55 W	0.71 W
Iron losses	251 W	215 W	230 W	200 W	127.7 W	126 W	177.6 W	162.2 W

- *PAM= Proposed Analytical Method

IX. CONCLUSION

In HSPM machines, the airgap field harmonics induce significant eddy current losses in the PM with the increase in rotating speed, which can increase the temperature and demagnetize the PM as well as affect the electromagnetic performance. Hence, in this paper, a new design with a solid PM rotor and titanium-based retaining sleeve was proposed to reduce the magnet eddy current losses in the HSPM machine. The performance of a two-pole/three-slot machine with non-overlapping winding was analyzed and the proposed model was compared with the conventional models. The PM eddy current loss was reduced by diminishing the undesirable harmonics of the airgap flux density. When compared with the conventional models, the airgap flux density harmonics demonstrated a lower amplitude in the proposed machine. The proposed model revealed not only reduced magnet eddy current losses but also low cogging torque and iron losses at different loaded conditions, while the rated torque was less than that of the conventional models. Therefore, the proposed model was optimized for increasing the rated torque. In the optimized model, the rated torque was increased when compared with that in the initially proposed and conventional designs.

REFERENCES

[1] J.-G. Lee, H.-K. Yeo, H.-K. Jung, T.-K. Kim, and J.-S. Ro, "Electromagnetic and thermal analysis and design of a novel-structured surface-mounted permanent magnet motor with high-power-density," *IET Electr. Power Appl.*, vol. 13, no. 4, pp. 472–478, Apr. 2019.

[2] S. Khan, S. S. H. Bukhari, and J.-S. Ro, "Design and analysis of a 4-kW two-stack coreless axial flux permanent magnet synchronous machine for low-speed applications," *IEEE Access*, vol. 7, pp. 173848–173854, 2019.

[3] D. Gerada, A. Mebarki, N. L. Brown, C. Gerada, A. Cavagnino, and A. Boglietti, "High-speed electrical machines: Technologies, trends, and developments," *IEEE Trans. Ind. Electron.*, vol. 61, no. 6, pp. 2946–2959, Jun. 2014.

[4] A. Tenconi, S. Vaschetto, and A. Vigliani, "Electrical machines for high-speed applications: Design considerations and tradeoffs," *IEEE Trans. Ind. Electron.*, vol. 61, no. 6, pp. 3022–3029, Jun. 2014.

[5] D. Tao, K. L. Zhou, F. Lv, Q. Dou, J. Wu, Y. Sun, and J. Zou, "Magnetic field characteristics and stator core losses of high-speed permanent magnet synchronous motors," *Energies*, vol. 13, no. 3, p. 535, Jan. 2020.

[6] B. Lu, N. Dai, G. Xu, S. Zhang, and J. Yang, "Design of the structure of the rotor containment sleeve for high-speed PM machine," in *Proc. 2nd IEEE Conf. Energy Internet Energy Syst. Integr. (EI2)*, Beijing, China, Oct. 2018, pp. 1–5.

[7] G. Narjes and B. Ponick, "Novel method for the determination of eddy current losses in the permanent magnets of a high-speed synchronous machine," in *Proc. 8th Int. Conf. Electr. Mach. (ICEM)*, Alexandroupoli, Greece, Oct. 2018, pp. 1285–1290.

[8] D. Ouamara and F. Dubas, "Permanent-magnet eddy-current losses: A global revision of calculation and analysis," *Math. Comput. Appl.*, vol. 24, no. 3, p. 67, Jul. 2019.

[9] C. Di, I. Petrov, and J. J. Pyrhönen, "Extraction of rotor eddy-current harmonic losses in high-speed solid-rotor induction machines by an improved virtual permanent magnet harmonic machine model," *IEEE Access*, vol. 7, pp. 27746–27755, 2019.

[10] G. Berardi and N. Bianchi, "High-speed PM generators for organic rankine cycle systems: Reduction of eddy current rotor losses," *IEEE Trans. Ind. Appl.*, vol. 55, no. 6, pp. 5800–5808, Nov. 2019.

[11] K. Yamazaki, Y. Fukushima, and M. Sato, "Loss analysis of permanent magnet motors with concentrated Windings–Variation of magnet eddy current loss due to stator and rotor shapes," in *Proc. IEEE Ind. Appl. Soc. Annu. Meeting*, Edmonton, AB, Canada, Oct. 2008, pp. 1–8.

[12] H.-K. Yeo and J.-S. Ro, "Novel analytical method for overhang effects in surface-mounted permanent-magnet machines," *IEEE Access*, vol. 7, pp. 148453–148461, 2019.

[13] M. Merdzan, J. J. H. Paulides, and E. A. Lomonova, "Comparative analysis of rotor losses in high-speed permanent magnet machines with different winding configurations considering the influence of the inverter PWM," in *Proc. 10th Int. Conf. Ecological Vehicles Renew. Energies (EVER)*, Monte Carlo, Monaco, Jun. 2015, pp. 1–8.

[14] S. Spas, G. Dajaku, and D. Gerling, "Eddy current loss reduction in PM traction machines using two-tooth winding," in *Proc. IEEE Vehicle Power Propuls. Conf. (VPPC)*, Montreal, QC, Canada, Dec. 2015, pp. 1–6.

[15] O. Payza, Y. Demir, and M. Aydin, "Investigation of losses for a concentrated winding high-speed permanent magnet-assisted synchronous reluctance motor for washing machine application," *IEEE Trans. Magn.*, vol. 54, no. 11, pp. 1–5, Nov. 2018.

[16] K. Yamazaki and H. Ishigami, "Rotor-shape optimization of interior-permanent-magnet motors to reduce harmonic iron losses," *IEEE Trans. Ind. Electron.*, vol. 57, no. 1, pp. 61–69, Jan. 2010.

[17] J.-X. Shen, H. Hao, M.-J. Jin, and C. Yuan, "Reduction of rotor eddy current loss in high speed PM brushless machines by grooving retaining sleeve," *IEEE Trans. Magn.*, vol. 49, no. 7, pp. 3973–3976, Jul. 2013.

[18] A. M. Gabay, M. Marinescu-Jasinski, J. Liu, and G. C. Hadjipanayis, "Internally segmented Nd-Fe-B/CaF_2 sintered magnets," *IEEE Trans. Magn.*, vol. 49, no. 1, pp. 558–561, Jul. 2012.

[19] Y. Wang, J. Ma, C. Liu, G. Lei, Y. Guo, and J. Zhu, "Reduction of magnet eddy current loss in PMSM by using partial magnet segment method," *IEEE Trans. Magn.*, vol. 55, no. 7, pp. 1–5, Jul. 2019.

[20] W.-Y. Huang, A. Bettayeb, R. Kaczmarek, and J.-C. Vannier, "Optimization of magnet segmentation for reduction of eddy-current losses in permanent magnet synchronous machine," *IEEE Trans. Energy Convers.*, vol. 25, no. 2, pp. 381–387, Jun. 2010.

[21] O. de la Barriere, S. Hlioui, H. B. Ahmed, and M. Gabsi, "An analytical model for the computation of no-load eddy-current losses in the rotor of a permanent magnet synchronous machine," *IEEE Trans. Magn.*, vol. 52, no. 6, pp. 1–13, Jun. 2016.

[22] W. Wu, J. Si, H. Feng, Z. Cheng, Y. Hu, and C. Gan, "Rotor eddy current loss calculation of a 2DoF direct-drive induction motor," *Energies*, vol. 12, no. 6, p. 1134, Mar. 2019.
[23] M.-S. Sim and J.-S. Ro, "Analysis of an eddy current brake for an actuator of a high-voltage direct current circuit breaker," *IET Electric Power Appl.*, vol. 13, no. 9, pp. 1387–1391, Sep. 2019.
[24] M.-S. Sim and J.-S. Ro, "Semi-analytical modeling and analysis of Halbach array," *Energies*, vol. 13, no. 5, p. 1252, Mar. 2020.
[25] L. Weili, Q. Hongbo, Z. Xiaochen, and Y. Ran, "Influence of copper plating on electromagnetic and temperature fields in a high-speed permanent-magnet generator," *IEEE Trans. Magn.*, vol. 48, no. 8, pp. 2247–2253, Aug. 2012.
[26] B. Hannon, P. Sergeant, and L. Dupré, "Evaluation of the rotor eddy-current losses in high-speed PMSMs with a shielding cylinder for different stator sources," *IEEE Trans. Magn.*, vol. 55, no. 3, pp. 1–10, Mar. 2019.
[27] L. Pei, L. Li, Q. Guo, R. Yang, and P. Du, "A novel rotor eddy current loss estimation method for permanent magnet synchronous machines with small inductance and a conductive rotor sleeve," *Energies*, vol. 12, no. 19, p. 3760, Sep. 2019.
[28] S. Chaithongsuk, N. Takorabet, and F. Meibody-Tabar, "On the use of pulse width modulation method for the elimination of flux density harmonics in the air-gap of surface PM motors," *IEEE Trans. Magn.*, vol. 45, no. 3, pp. 1736–1739, Mar. 2009.
[29] Z. Belli, "Optimization of stator slots shape for eddy current losses reduction in permanent magnets synchronous machine," in *Proc. 9th Int. Conf. Ecological Vehicles Renew. Energies (EVER)*, Monte-Carlo, Monaco, Jun. 2014, pp. 1–7.
[30] G. Zhang, F. Wang, and Y. Shen, "Reduction of rotor loss and cogging torque of high speed PM machine by stator teeth notching," in *Proc. IEEE Int. Conf. Electr. Mach. Syst. (ICEMS)*, Seoul, South Korea, Dec. 2007, pp. 856–859.
[31] J. Ma and Z. Q. Zhu, "Magnet eddy current loss reduction in permanent magnet machines," *IEEE Trans. Ind. Appl.*, vol. 55, no. 2, pp. 1309–1320, Mar. 2019.
[32] D. K. Hong, B. C. Woo, and D. H. Koo, "Rotordynamics of 120 000 r/min 15 kW ultra high speed motor," *IEEE Trans. Magn.*, vol. 45, no. 6, pp. 2831–2834, May 2009.
[33] H. Fang, D. Li, R. Qu, J. Li, C. Wang, and B. Song, "Rotor design and eddy-current loss suppression for high-speed machines with a solid-PM rotor," *IEEE Trans. Ind. Appl.*, vol. 55, no. 1, pp. 448–457, Jan. 2019.
[34] Z. Zhu, Y. Huang, J. Dong, F. Peng, and Y. Yao, "Rotor eddy current loss reduction with permeable retaining sleeve for permanent magnet synchronous machine," *IEEE Trans. Energy Convers.*, vol. 35, no. 2, pp. 1088–1097, Jun. 2020.
[35] W. Li, H. Qiu, X. Zhang, J. Cao, S. Zhang, and R. Yi, "Influence of rotor-sleeve electromagnetic characteristics on high-speed permanent-magnet generator," *IEEE Trans. Ind. Electron.*, vol. 61, no. 6, pp. 3030–3037, Jun. 2014.
[36] R. Deeb, "Calculation of eddy current losses in permanent magnets of servo motor," in *Proc. 17th Annu. Student Conf. Competition (STUDENT EEICT)*, Brno, Czech Republic, Jun. 2011.
[37] Z.-Q. Zhu, S. Xue, W. Chu, J. Feng, S. Guo, Z. Chen, and J. Peng, "Evaluation of iron loss models in electrical machines," *IEEE Trans. Ind. Appl.*, vol. 55, no. 2, pp. 1461–1472, Apr. 2019.
[38] L. Ur Rahman, F. Khan, M. A. Khan, N. Ahmad, H. A. Khan, M. Shahzad, S. Ali, and H. Ali, "Modular rotor single phase field excited flux switching machine with non-overlapped windings," *Energies*, vol. 12, no. 8, p. 1576, Apr. 2019.

HAMID ALI KHAN received the B.S. and M.S. degrees in electrical engineering from COMSATS University Islamabad–Attock and Abbottabad, Pakistan, in 2017 and 2020, respectively.

He was a Researcher with the Electric Machine Design Research Laboratory, Electrical and Computer Engineering Department, COMSATS University Islamabad–Abbottabad, from 2017 to 2020, focuses on designing and analysis of high speed electrical machines. He has been a Visiting Researcher with the College of Mechatronics and Control Engineering, Shenzhen University, Shenzhen, China, since 2019. His research interests include design, analysis and optimization of high speed electrical machines, permanent magnet synchronous machines, flux switching machines, and DC machines.

FAISAL KHAN was born in Utmanzai, Charsadda, Khyber Pakhtunkhwa, Pakistan, in 1986. He received the B.S. degree in electronics engineering and the M.S. degree in electrical engineering from the COMSATS Institute of Information Technology Islamabad–Abbottabad, Pakistan, in 2009 and 2012, respectively, and the Ph.D. degree in electrical engineering from Universiti Tun Hussein Onn Malaysia, Malaysia, in 2017.

From 2010 to 2012, he was a Lecturer with the University of Engineering & Technology Peshawar–Abbottabad, Pakistan. Since 2017, he has been an Assistant Professor with the Electrical and Computer Engineering Department, COMSATS University Islamabad–Abbottabad, Pakistan. He is currently the Head of the Electric Machine Design Research Laboratory, Electrical and Computer Engineering Department, COMSATS University Islamabad–Abbottabad. He is the author of more than 80 publications and received multiple research awards. His research interests include design of flux-switching, synchronous, induction, linear, and DC machines.

NASEER AHMAD was born in Lakki Marwat, Khyber Pakhtunkhwa (KPK), Pakistan, in 1992. He received the bachelor's degree in electrical power engineering from the University of Engineering and Technology Peshawar, in 2015, and the M.S. degree in electrical engineering COMSATS University Islamabad–Abbottabad, Pakistan, in 2018.

He has been a Lecturer with the Electrical Engineering Department, Balochistan University of Information Technology, Engineering and Management Sciences (BUITEMS), Quetta, Pakistan, since October, 2019. His research interests are design and optimization of outer rotor flux switching machine, flux reversal machines, and synchronous machines.

JONG-SUK RO received the B.S. degree in mechanical engineering from Han-Yang University, Seoul, South Korea, in 2001, and the Ph.D. degree in electrical engineering from Seoul National University (SNU), Seoul, in 2008.

In 2014, he was with the University of BATH, Bath, as UK an Academic Visitor. From 2013 to 2016, he worked with the Brain Korea 21 Plus, SNU, as a BK Assistant Professor. He conducted research at the Electrical Energy Conversion System Research Division, Korea Electrical Engineering & Science Research Institute as a Researcher, in 2013. From 2012 to 2013, he was with the Brain Korea 21 Information Technology of SNU, as a Postdoctoral Fellow. He conducted research at the Research and Development Center of Samsung Electronics as a Senior Engineer, from 2008 to 2012. He is currently an Associate Professor with the School of Electrical and Electronics Engineering, Chung-Ang University, Seoul. His research interests include the analysis and optimal design of next-generation electrical machines using smart materials, such as electromagnet, piezoelectric, magnetic shape memory alloy, and so on.